Corrosion Inhibition of Mild Steel in 1.0 M HCl by two Hydrazone Derivatives

H. Lgaz [1], S. Zehra [2], M. R. Albayati [3], K. Toumiat [4], Y. El Aoufir [5], A. Chaouiki [6], R. Salghi [6], Ismat. H. Ali [7], M. I. Khan [8], I-M. Chung [1*], S. K. Mohamed [9]*

[1] Department of Crop Science, College of Sanghur Life Science, Konkuk University, Seoul 05029, South Korea
[2] Corrosion Research Laboratory, Department of Applied Chemistry, Faculty of Engineering and Technology, Aligarh Muslim University, Aligarh, India
[3] Department of Chemistry, College of Education, Kirkuk University, Kirkuk, Iraq
[4] Department of Materials Sciences, Laghouat University, PO Box 37, 03000, Laghouat, Algeria
[5] Materials, Nanotechnology and Environment Laboratory, Faculty of Sciences, Mohammed V University Rabat, Morocco.
[6] Laboratory of Applied Chemistry and Environment, ENSA, University Ibn Zohr, PO Box 1136, Agadir, Morocco
[7] Department of Chemistry, College of Science, King Khalid University, P. O. Box 9004, Postal Code 61413, Abha, Kingdom of Saudi Arabia
[8] Chemical Engineering Department, College of Engineering, King Khalid University, Abha, Kingdom of Saudi Arabia
[9] Faculty of Science and Engineering, Health Care Division, Manchester Metropolitan University, Manchester M1 5GD, England
[*]E-mail: r.salghi@uiz.ac.ma, imcim@konkuk.ac.kr

In this paper, a combined experimental and theoretical study was conducted to explain the scientific mechanism of adsorption of two hydrazone derivatives (HDZs) containing mefenamic acid (MA) namely, (E)-2-((2,3-dimethylphenyl)amino)-N'-(thiophen-2-ylmethylene)benzohydrazide (HDZ-S) and (E)-2-((2,3-dimethylphenyl)amino)-N'-(furan-2-ylmethylene)benzohydrazide (HDZ-O) on mild steel (MS) in 1.0 M HCl. Electrochemical techniques and scanning electron microscope (SEM) were performed to evaluate the corrosion inhibition performances. Electrochemical results disclosed that the two compounds could effectively control the dissolution rate of mild steel in acidic medium through physicochemical adsorption following Langmuir adsorption model. Potentiodynamic polarization curves indicated that the furocoumarin molecules could be classified as mixed-type inhibitors by preventing anodic metal dissolution and cathodic hydrogen evolution reaction. The results of SEM experiment agree with electrochemical results and confirm the effective adsorption of both compounds on the steel surface.

1. INTRODUCTION

An impressive and growing amount of research has been devoted to understanding the corrosion of steel and its alloys[1–5] due to its great importance in several engineering applications [6]. However, the main disadvantage of these steels is their highest susceptibility to corrosion when exposed to an acidic media. In today's world, the use of hydrochloric acid solution in many industrial processes (e. g. cleaning, pickling, descaling) is of increasing importance in order to save energy and money[7]. Adding corrosion inhibitors to these acidic environments is the specially common and effective way to prevent the dissolution of metal[8,9]. Heterocyclic compounds containing electron rich functional groups, heteroatom like N, O and S along with aromatic rings and unsaturated π-bonds often show good corrosion inhibitive properties in acid media[10–12]. The inhibitive effect of these groups is attributable to their adsorption centers, which ensure high interaction with metal surface by either chemisorption or physisorption or both, thus leading to the formation of a protective layer. Making use of natural products or synthesized green organic compounds completely replace toxic inhibitors like chromates plays an important role in promoting sustainable development of environment [13–16].

Hydrazones represent an extremely versatile class of compounds in heterocyclic chemistry because of their wide range of applications such as antimicrobial [17], antiviral [18], anti-cancer drugs [19–21] and new anti-corrosive agents [22–24].
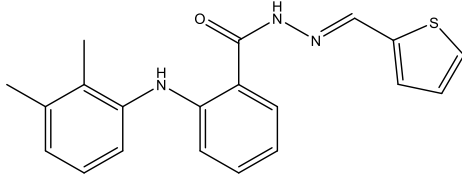
The central aim of this paper is to assess the extent to which two hydrazone compounds have contributed to mild steel protection by applying experimental techniques, i.e. electrochemical and weight loss as well as surface characterization techniques, i.e. SEM.

2. MATERIALS AND METHODS

2.1. Inhibitors

The hydrazone derivatives used in the present study were synthesized according to the procedure published in our recent papers [23,25]. Both compounds contain several heteroatoms and aromatic rings, which motivate us to study their corrosion inhibition for mild steel in 1.0 M HCl. Molecular structures, names and abbreviation of tested compounds are given in Table 1.

Table 1. Chemical names and structures of tested inhibitors.

name	Structure	Notation
(E)-2-((2,3-dimethylphenyl)amino)-N'-(thiophen-2-ylmethylene)benzohydrazide		HDZ-S

| (E)-2-((2,3-dimethylphenyl)amino)-N'-(furan-2-ylmethylene)benzohydrazide | | HDZ-O |
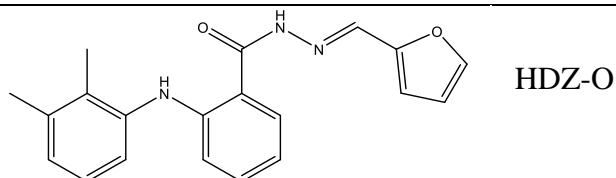
2.2. Materials and corrosive solutions

Metal sheet of steel of commercial purpose which has the following composition: 0.36 C, 0.66 Mn, 0.27 Si, 0.02 S, 0.015 P, 0.21 Cr, 0.02 Mo, 0.22 Cu, 0.06 Al, and balance Fe, was used for performing all kinds of the experimental work. Surface of MS specimens were grated with different degrees of granulation of abrasive papers (SiC; 600-1600), the abraded specimens were cleansed with bidistilled water, then with acetone, and eventually dried at room temperature. The test solution employed (HCl of 1.0 M concentation) was prepared from the commercially obtained 37% HCl, by diluting with aid of distilled water.

2.3. Weight loss measurements

Weight loss tests were performed according to procedure detailed in our previous works [26]. All tests were performed respecting the standard laboratory methodology adopted by the ASTM [27]. For each concentration, triplicates measurements were carried out. The corrosion rate (C_{RW}) in millimeters per year (mm y^{-1}) was calculated by dividing the mass loss (W) in gram by the exposed area (A) in cm^2, density (7.86 g cm^{-3}) [28], and time of exposure in hours using the following equation [29]:

$$C_{RW} = \frac{K \times W}{A \times t \times \rho} \qquad (1)$$

where K= 8.76×10^4 was used as constant.

Equations (2) and (3) were used to estimate the inhibition efficiency $\eta_{WL}(\%)$ and the surface coverage (θ) of investigated compounds [30]:

$$\eta_{WL}(\%) = \left[\frac{C_{RW}^{\circ} - C_{RW}}{C_{RW}^{\circ}}\right] \times 100 \qquad (2)$$

$$\theta = \left[\frac{C_{RW}^{\circ} - C_{RW}}{C_{RW}^{\circ}}\right] \qquad (3)$$

where C_{RW}° and C_{RW} are respectively the corrosion rates in absence and in presence of inhibitor's concentration.

2.3. Electrochemical measurements

Electrochemical experiments were carried out by using an electrochemical workstation (Tacussel Radiometer PGZ 100 potentiostat) controlled by VoltaMaster software, and a cell of glass consisting of three electrodes i.e. working electrode (mild steel), reference electrode (saturated calomel electrode (SCE)), and counter electrode (platinum) were used for the all the corrosion reactions. After the attainment of steady state open circuit potential (OCP) by the working electrode that took around a half

hour after exposure, electrochemical curves were recorded. EIS tests were carried out by the application of peak-to-peak perturbations of 5 mV, at open circuit potential in the frequency range 10 mHz to 100 KHz. PDP curves reported here were obtained at a scan rate of 1 mVs^{-1} by automatically sweeping the applied electrode potential from -800 to -200 mV vs. OCP. Tafel extrapolation method was used to extract electrochemical parameters at ± 50 mV around E_{corr} [31].

2.6. Surface characterization

The surface morphology of the mild steel samples were characterized with scanning electron microscopy in the absence and presence of 5×10^{-3} M of inhibitors. SEM imaging was performed on samples after a 6h immersion time. A Hitachi TM-1000 SEM at an accelerating voltage of 15 kV was used for SEM analysis.

3. RESULTS AND DISCUSSION

3.1. Weight loss measurements

Table 2 illustrates various corrosion inhibition parameters of mild steel in 1 M HCl under inhibited and uninhibited conditions at 303K, which are obtained from gravimetric measurements:

Table 2. Weight loss data of MS in uninhibited and inhibited solutions at 303 K.

Inhibitors	Concentration/ M	C_{RW}/ mm y^{-1}	η_{WL}/ %
HCl	1	130.4	-
HDZ-O	1×10^{-4}	51.1	60
	5×10^{-4}	33.1	74
	1×10^{-3}	24.7	81
	5×10^{-3}	12.3	90
HDZ-S	1×10^{-4}	45.7	64
	5×10^{-4}	29.5	77
	1×10^{-3}	19.3	85
	5×10^{-3}	10.5	92

As shown in Table 1, the addition of inhibitors to the aggressive solution reduced the corrosion rates of mild steel markedly. The inhibition efficiency increases with increasing inhibitor concentration, with maximum of 92% and 90% at 5×10^{-3} M concentration of HDZ-S and HDZ-O respectively, representing an excellent inhibition performance of HDZ-S compared to HDZ-O towards the mild steel corrosion. These results can be attributed to the quick adsorption of hydrazone derivatives on the mild

steel surface, because of the presence of several reactive sites like heteroatoms (N, O and S), π-electrons and aromatic rings, which can greatly facilitate the adsorption of inhibitors onto the steel surface.

3. 2. Electrochemical techniques

Concentration effect of HDZs on the polarization behavior of mild steel in 1.0 M HCl was analyzed and the Tafel plots were recorded for different inhibitor concentrations and represented in Figure 1.
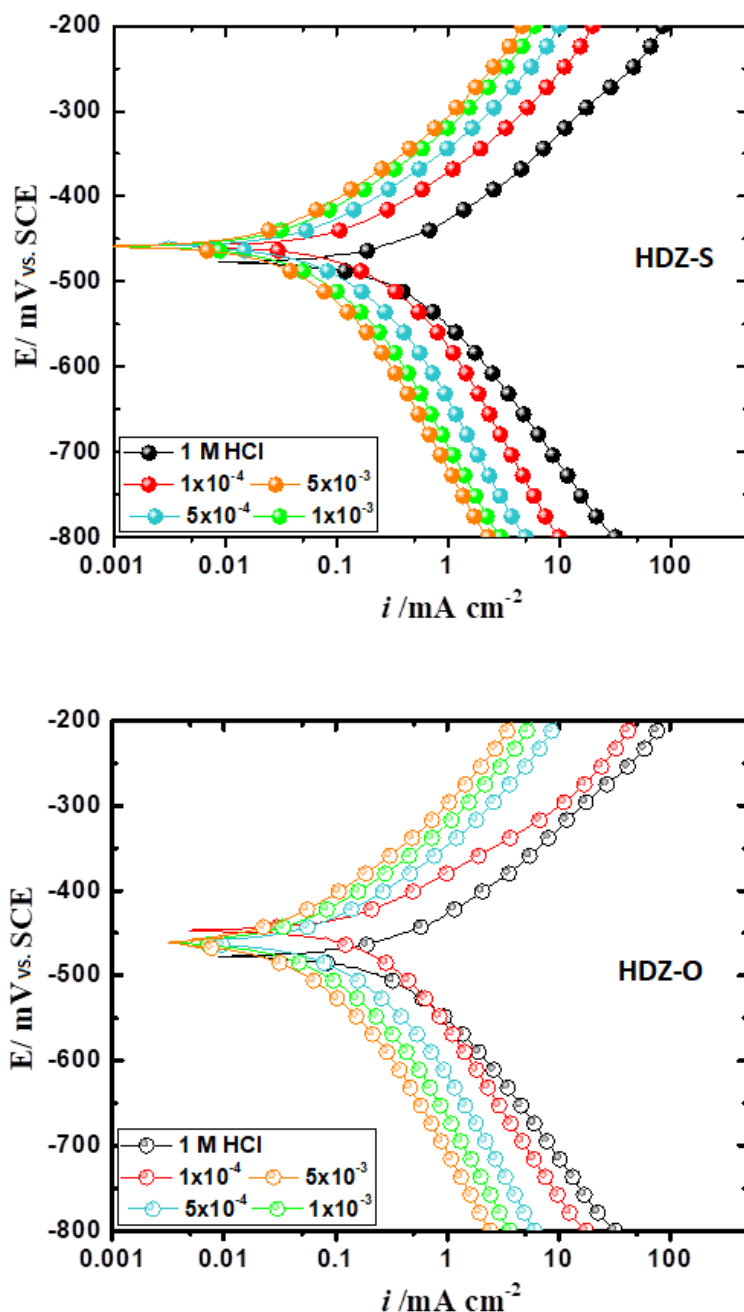

Figure 1. PDP curves of mild steel in 1.0 M HCl with and without inhibitor concentrations at 303 K.

Table 3 lists some electrochemical corrosion parameters. The following equation was used to estimate the inhibition efficiencies of tested compounds [32]:

$$\eta_{PDP}(\%) = \left[1 - \frac{i_{corr}}{i^\circ_{corr}}\right] \times 100 \qquad (4)$$

where i_{corr} and i°_{corr} are the corrosion current densities with and without inhibitors,

It is apparently obvious from Figure 1 that the addition of both inhibitors to the HCl solution considerably reduces the cathodic and anodic current densities and enhances the corrosion resistance of the mild steel even at low inhibitor concentrations. From polarization data of the inhibitors, E_{corr} values showed no deviation towards the positive or negative sides. In case the displacement from blank E_{corr} is less than 85mV, compounds are expected to behave as mixed type of inhibitors. Overall, these results indicate that these compounds are mixed type inhibitors i.e., the addition of each inhibitor effectively retarded the corrosion reaction without changing the mechanism of corrosion process[33]. Results from Table 3 reveal that the i_{corr} values is decreasing continuously with increasing inhibitor concentration, suggesting that both hydrazone derivatives successfully inhibited the reactions of both cathodic and anodic behaviors. The decreased values of i_{corr} in presence of inhibitors is attributable towards enhanced effectiveness. This effectiveness is due to the blocking effect by inhibitors of corrosion active sites [34] resulted from their adsorption onto the mild steel surface. From Table 3, it is clear that the βc and βa remains almost unchanged, which indicates the inhibitors' molecule act as adsorptive inhibitor [35]. Evidently, $\eta_{PDP}(\%)$ increased by increasing the inhibitors' concentration and reaches up to 89% and 85% at 5×10^{-3} M for HDZ-S and HDZ-O respectively. This indicated their effectiveness against the mild steel corrosion in the acid media.

Table 3. The parameters of PDP of the MS in uninhibited and inhibited solutions at 303 K.

Inhibitors	Concentration/ M	$-E_{corr}$ / mV SCE^{-1}	$-\beta_c$ / mV dec^{-1}	β_a / mV dec^{-1}	i_{corr} / $\mu A\ cm^{-2}$	η_{PDP} / %	Θ
HCl	1.0	480	175	116	481	-	-
HDZ-O	1×10^{-4}	450	166	101	245	48	0.48
	5×10^{-4}	467	183	109	155	67	0.67
	1×10^{-3}	463	170	111	97	79	0.79
	5×10^{-3}	466	185	104	70	85	0.85
HDZ-S	1×10^{-4}	463	188	109	213	55	0.55
	5×10^{-4}	459	179	104	105	78	0.78
	1×10^{-3}	454	181	98	77	84	0.84
	5×10^{-3}	456	184	100	53	89	0.89

Figures 2 and 3 present the results of mild steel experimental impedance in 1 M HCl without and with different concentrations of tested hydrazone derivatives. Figure 2 shows the Nyquist plots while the Bode plots (for optimum concentration) are shown in Figure 3.
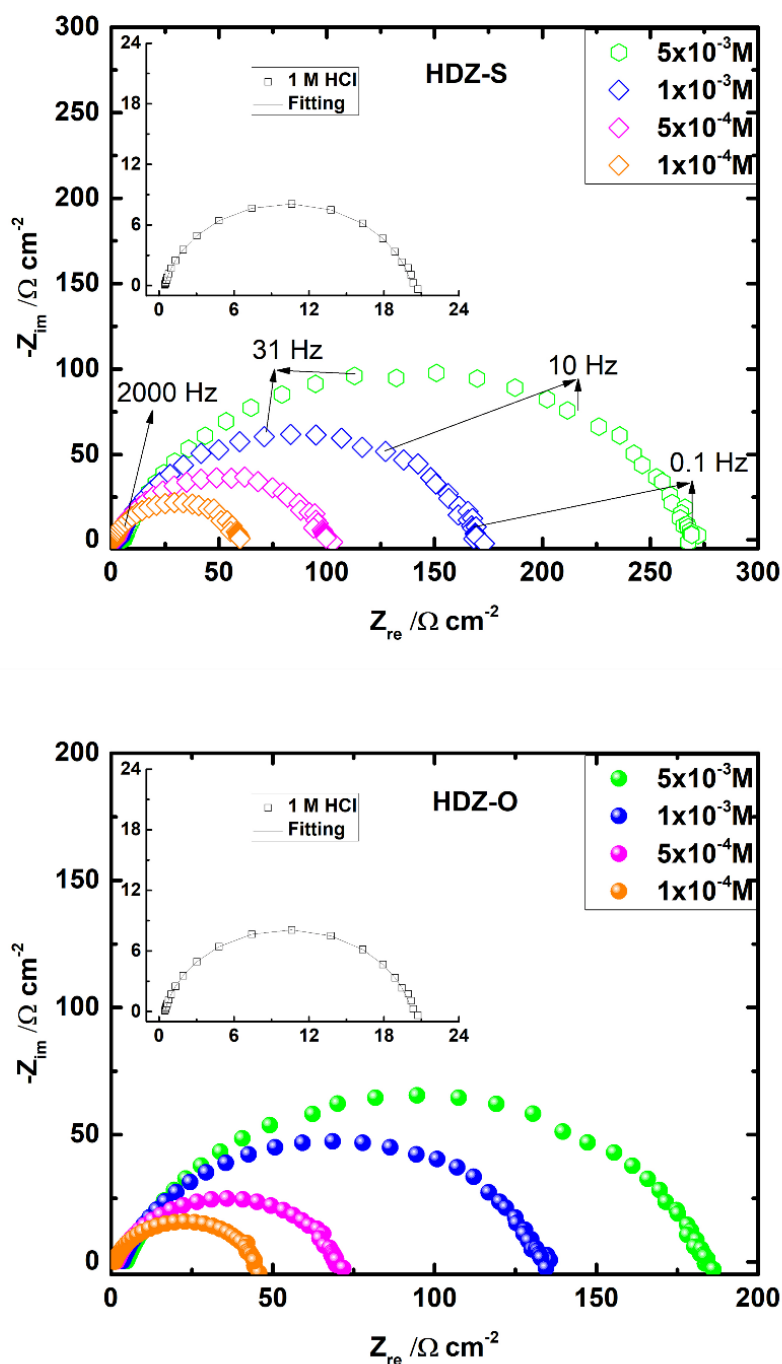
Figure 2. Nyquist diagrams of mild steel in 1.0 M HCl with and without inhibitor concentrations at 303 K.

It is observable that at higher frequency region, the plots exhibited one single capacitive loop somewhat depressed at the center which signified that corrosion of mild steel in 1.0 M HCl solution is

mainly governed by charge transfer mechanism [36]. All Nyquist curves exhibit single depressed semicircles which is due to the fact that the double layer at metal/solution interface usually displaying a non-ideal capacitive behavior which is known as the frequency dispersion[37]. This is usually due to different phenomenon like non-homogeneity, impurities, surface roughness of the mild steel [38]. The impedance data were fitted to the electrical equivalent circuit shown in Figure 4 to extract the impedance parameters from the experimental results [39,40]. More details on the CPE and the used equivalent circuit model are given in our previous works [41].

The interfacial capacitance C_{dl} can be calculated from the polarization resistance and CPE parameter values Q and n using the expression[42]:

$$C_{dl} = \sqrt[n]{Q \times R_p^{1-n}} \tag{5}$$

Table 4 lists electrochemical impedance parameters while the following equation was used to estimate the inhibitive performance[43]:

$$\eta_{EIS}(\%) = \left[\frac{R_{p(inh)} - R_p}{R_{p(inh)}} \right] \times 100 \tag{6}$$

where, $R_{p(inh)}$ and R_p are polarization resistances with and without inhibitors, respectively.
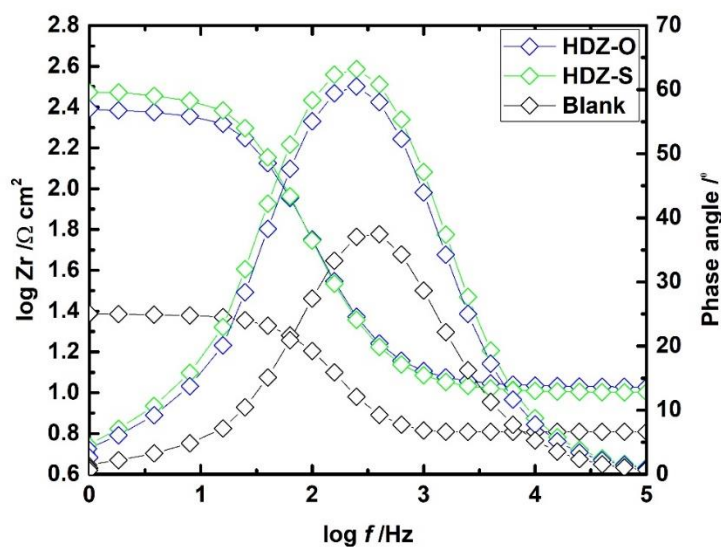
Figure 3. Bode ($\log f$ *vs.* $\log |Z|$) and phase angle ($\log f$ *vs.* Φ) plots of impendence spectra for MS in 1 M HCl and containing 5×10^{-3} M of inhibitors.
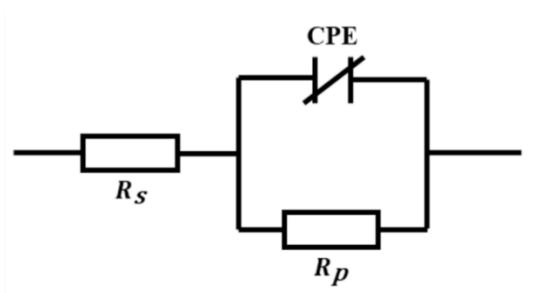
Figure 4. The electrochemical equivalent circuit.

According to the data given in Table 4, the R_p data of inhibited substrates gets enhanced as the concentration of inhibitors goes uphill. Moreover, the values of C_{dl} are diminished as the each of the inhibitor dosage increases, which widely might happen due to the decreased local dielectric constant and/or increased double layer thickness. Overall, these results strengthen the idea that these compounds act via an effective adsorption at the interface between the metal and the solution i.e, as adsorptive inhibitors[44]. Evidently, $\eta_{PDP}(\%)$ increased by increasing the inhibitor concentration and reaches up to 92% and 88% at 5×10^{-3} M for HDZ-S and HDZ-O respectively. This indicated the effectiveness of both compounds against the mild steel corrosion in the acid media.

Table 4. Impedance parameters for corrosion of MS in uninhibited and inhibited solutions at 303 K.

Inhibitors	Concentration/ M	R_p/ $\Omega\ cm^2$	n	$Q\times10^{-4}$/ $S^n\ \Omega^{-1}\ cm^{-2}$	C_{dl}/ $\mu F\ cm^{-2}$	η_{EIS}/ %
Blank	1.0	20.24	0.860	2.420	112.04	-
HDZ-O	1×10^{-4}	45	0.83	1.3016	45	55
	5×10^{-4}	68	0.83	1.0045	36	70
	1×10^{-3}	130	0.80	0.8987	29	84
	5×10^{-3}	179	0.81	0.7313	26	88
HDZ-S	1×10^{-4}	58	0.82	1.0563	34	65
	5×10^{-4}	97	0.85	0.7389	31	79
	1×10^{-3}	166	0.86	0.5114	23	87
	5×10^{-3}	264	0.83	0.4555	18	92

3.3. Adsorption isotherm

The adsorption isotherms were used to gain basic information on the interaction between hydrazones and mild steel surface. The calculated values of surface coverage (θ) obtained from weight loss tests could fit into the various adsorption isotherm equations. The best fit was modeled for the Langmuir isotherm model (defined by eq. 7) [45]:

$$\frac{C_{inh}}{\theta} = \frac{1}{K_{ads}} + C_{inh} \qquad (7)$$

Where K_{ads} is the adsorption-desorption equilibrium constant, C_{inh} is the concentration of the inhibitors in the solution. In addition, the K_{ads} can be determined by the intercept of straight line. The free energy of adsorption ΔG_{ads}° was calculated using the values of K_{ads} by the Equation 8:

$$\Delta G_{ads}^{\circ} = -RT\ln(K_{ads} \times C_{solvent}) \qquad (8)$$

where, K_{ads} is the rate constant, R as a gas constant and T is Kelvin temperature. ΔG_{ads}° was calculated and tabulated in Table 5 for the two inhibitor molecules while Figure 5 represents the plot of

Langmuir model. The slopes of the straight lines are 1.05 and 1.06 for HDZ-S and HDZ-O respectively, suggesting that there are no interactions among the adsorbed inhibitor molecules at the mild steel surface. A considerable amount of literature [46–51] reveals that the values of ΔG_{ads}° up to -20 kJ/mol or less negative are usually associated with the physical adsorption process while those around or higher (more negative) than -40 kJ/mol with the chemical adsorption process [52]. In the present study, ΔG_{ads}° values are between -20 kJ mol^{-1} and -40 kJ mol^{-1}, which means a mixed type of adsorption through physical and chemical adsorption [36].
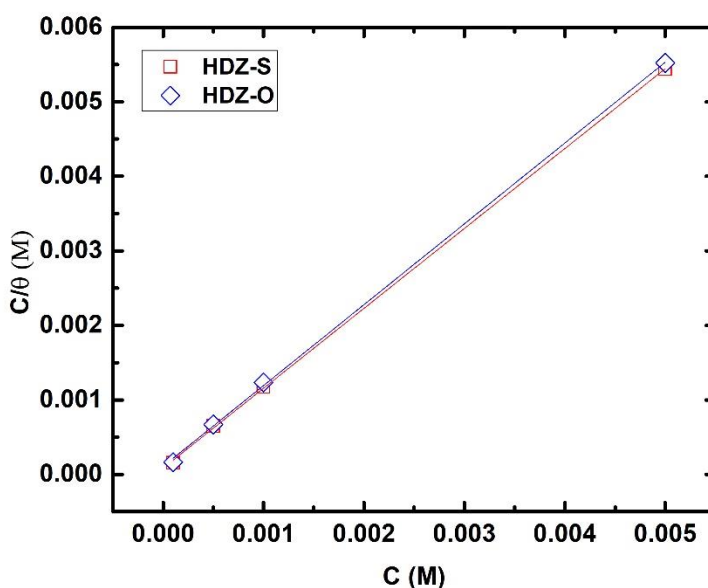
Figure 5. Plots of the Langmuir adsorption isotherm of inhibitors at 303 K.

Table 5. The adsorption parameters for the corrosion of MS in inhibited solutions at 303 K.

Inhibitor	Slope	K_{ads} (M^{-1})	R^2	ΔG_{ads}° (kJ mol^{-1})
HDZ-S	1.05	11819	0.999	-37
HDZ-O	1.06	9260	0.999	-34

3.4. Scanning electron microscope

Scanning electron microscope was used to study the surface morphology of the mild steel surface exposed to 1.0 M HCl without and with 5×10^{-3} M of HDZ-S and HDZ-O for 6h immersion. As shown in Figure 6(A), the surface of the mild steel in absence of inhibitor is highly corroded and damaged due to metal dissolution. In contrast, smoother surface was observed in the presence of inhibitors as clearly observed in Figure 6(B) and Figure 6(C). The improved surface morphology of steel surface is due to better adsorption of inhibitors on the mild steel surface.
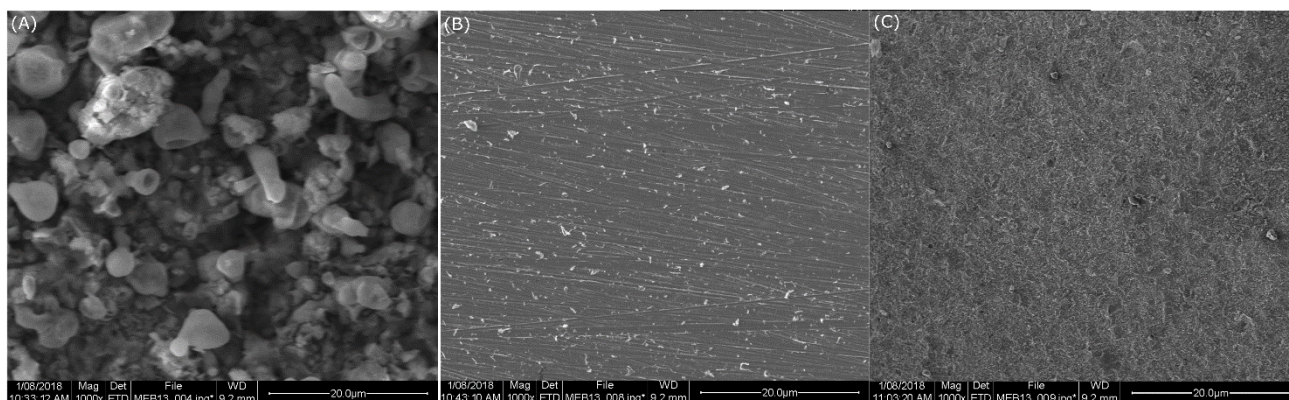
Figure 6. SEM images of MS in (A) 1.0 M HCl and in 1.0 M HCl + 5×10^{-3} M of (B) HDZ-S and (C) HDZ-O after 6h of immersion time.
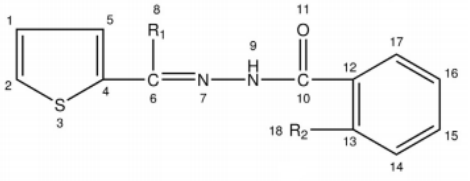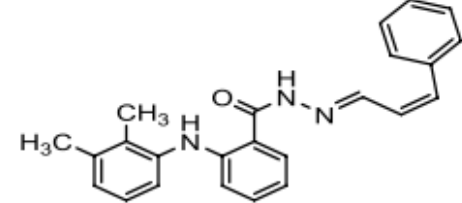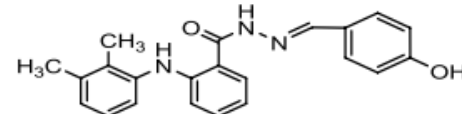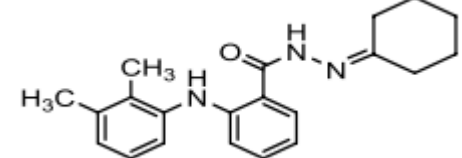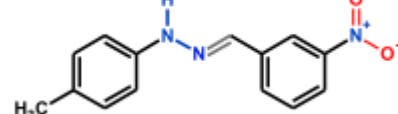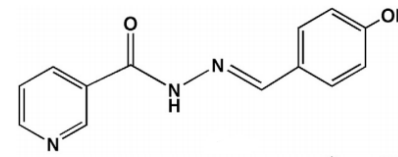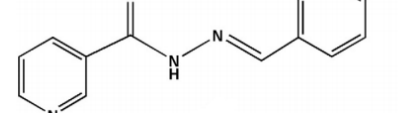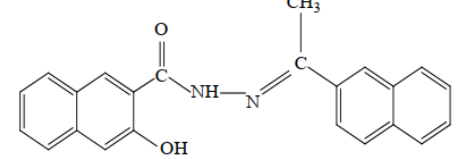
3.7. Mechanism of adsorption and inhibition

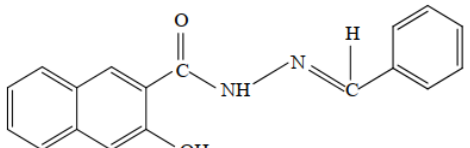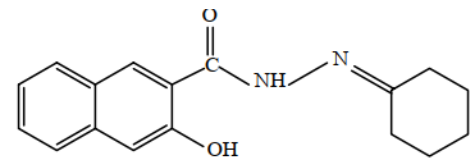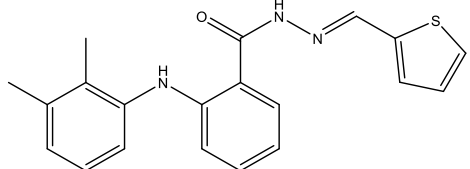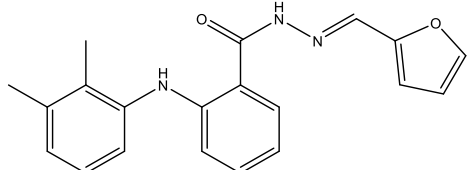The choice of investigated compounds was encouraged by the presence of functional groups in their molecular structure as well as the efficacy of similar compounds [23,25]. The functional groups mainly increase the thickness of the protective film on the surface of the metal and hinder the metal corrosion rate in acid solution. As expected, the results obtained in the present study show that both tested compounds have a great tendency to protect mild steel, which is mainly due to the presence of heteroatoms and π-bonds as well as the planarity of their molecular structure. Both compounds can preferentially protonated in 1 M HCl, which can favorite electrostatic interactions with charged metal surface with chlorine ions as intermediates. Other form of interaction is through electron sharing between free electron pairs of heteroatoms and π-electron from the aromatic rings and the iron atoms via its vacant *d*-orbital. The accumulation of negative charge on steel surface leads to the formation of back-donation interactions, which mean the transfer of electron from metal surface to inhibitor molecule.

3.8. Comparison of similar compounds in literature

Recently, many studies have been carried out in order to find efficient and environmentally safe corrosion inhibitors for mild steel corrosion, so that many compounds have been developed [23, 25, 53–58]. Table 6 compares the inhibition performance of tested hydrazones with selected similar compounds used as corrosion inhibitors for steels in HCl and H_2SO_4 mediums. Data in Table 6 provide strong evidence that most of the hydrazones exhibited good inhibition efficiency. Hydrazone derivatives show good inhibitive performances for steels corrosion in HCl and H_2SO_4, which explains the recent interest in developing new hydrazone derivatives. In addition, the results show that our tested hydrazones provide good inhibition efficiency with respect to those provided by other hydrazone derivatives listed in Table 6. However, further improvement can be made to increase their inhibition efficiency through synergizing with halide ions or functionalization by other functional groups.

Table 6. Quantitative comparison of the inhibition efficiency of our compounds with similar hydrazone derivatives studied previously.

Inhibitor	Metal/Medium	Inhibition efficiency (%)/ Reference
R_1= CH_3, R_2= H; **ATBH**	Mild steel/ 0.5 M H_2SO_4	90.0 [53]
R_1= CH_2CH_3, R_2= H; **PTBH**		92.7 [53]
R_1= CH_3, R_2= NH_2; **ATABH**		93.7 [53]
R_1= CH_2CH_3, R_2= NH_2; **ATABH**		96.3 [53]
	Mild steel/ 1.0 M HCl	97.0 [23]
	Mild steel/ 1.0 M HCl	94.0 [23]
	Mild steel/ 1.0 M HCl	86.0 [23]
	Mild steel/ 1.0 M HCl	92.0 [23]
	Carbon steel/ 0.5 M H_2SO_4	86.41 [59]
	Mild steel/ 1.0 M HCl	95.5 [60]
	Mild steel/ 1.0 M HCl	96.6 [60]
	Carbon steel/ 0.5 M H_2SO_4	59 [58]
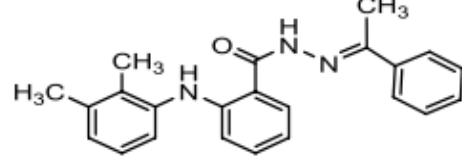
	Carbon steel/ 0.5 M H_2SO_4	56 [58]
	Carbon steel/ 0.5 M H_2SO_4	52 [58]
	Carbon steel/ 0.5 M H_2SO_4	50 [58]
	Mild steel/ 1.0 M HCl	92 [Present work]
	Mild steel/ 1.0 M HCl	88 [Present work]

4. CONCLUSION

Experimental and theoretical results indicate that both hydrazone compounds have good inhibitive properties for mild steel in 1.0 M HCl. Polarization studies have shown that the studied inhibitors work as mixed-type inhibitors. The adsorption of both inhibitors on the mild steel surface obeys the Langmuir adsorption isotherm. One of the strengths of this study is that it represents a comprehensive explanation of the corrosion inhibition performance of the synthesized compounds. Nevertheless, further theoretical investigation could also be conducted to study the reactivity of these compounds and the interaction mechanism with steel surface which will be addressed in next works.

References

1. Y. Zhang, Y. Cheng, F. Ma, K. Cao, *Int. J. Electrochem. Sci.* 14 (2019) 999.
2. F. Bentiss, M. Outirite, M. Traisnel, H. Vezin, M. Lagrenée, B. Hammouti, S.S. Al-Deyab, C. Jama, *Int. J. Electrochem. Sci.* 7 (2012) 1699.
3. M.A. Ameer, A.M. Fekry, A. Othman, *Int. J. Electrochem. Sci.* 9 (2014) 1964.
4. G. Khan, W.J. Basirun, A.B.B.M. Badry, S.N. Kazi, P. Ahmed, S.M. Ahmed, G.M. Khan, *Int. J. Electrochem. Sci.* 13 (2018) 12420.
5. X. Zhang, B. Tan, *Int. J. Electrochem. Sci.* 13 (2018) 11388.
6. A.B. da Silva, E. D'Elia, J.A. da C.P. Gomes, *Corros. Sci.* 52 (2010) 788.

7. A. Dutta, S.K. Saha, P. Banerjee, D. Sukul, *Corros. sci.* 98 (2015) 541.
8. O. Olivares-Xometl, C. López-Aguilar, P. Herrastí-González, N.V. Likhanova, I. Lijanova, R. Martínez-Palou, J.A. Rivera-Márquez, *Ind. Eng. Chem. Res.* 53 (2014) 9534.
9. N.K. Gupta, M.A. Quraishi, C. Verma, A.K. Mukherjee, *RSC Adv.* 6 (2016) 102076.
10. D.M. Gurudatt, K.N. Mohana, *Ind. Eng. Chem. Res.* 53 (2014) 2092.
11. A. El-Faham, S.M. Osman, H.A. Al-Lohedan, G.A. El-Mahdy, *Molecules,* 21 (2016) 714.
12. X. Gao, S. Liu, H. Lu, F. Gao, H. Ma, *Ind. Eng. Chem. Res.* 54 (2015) 1941.
13. C.B. Verma, M.A. Quraishi, A. Singh, *J. Taiwan Inst. Chem. Eng.* 49 (2015) 229.
14. M. Özcan, R. Solmaz, G. Kardaş, İ. Dehri, *Colloids Surf. Physicochem. Eng. Asp.* 325 (2008) 57.
15. V. Srivastava, J. Haque, C. Verma, P. Singh, H. Lgaz, R. Salghi, M.A. Quraishi, *J. Mol. Liq.* 244 (2017) 340.
16. A.Y. El-Etre, A.I. Ali, Chin. *J. Chem. Eng.* 25 (2017) 373.
17. M. Singh, N. Raghav, *Int. J. Pharm. Sci.* 3 (2011) 26.
18. P. Vicini, M. Incerti, P. La Colla, R. Loddo, *Eur. J. Med. Chem.* 44 (2009) 1801.
19. S. Rollas, S. Küçükgüzel, *Molecules,* 12 (2007) 1910.
20. N. Terzioglu, A. Gürsoy, *Eur. J. Med. Chem.* 38 (2003) 781.
21. R.M. Mohareb, J. Schatz, *Bioorg. Med. Chem.* 19 (2011) 2707.
22. M. Moussa, A. El-Far, A. El-Shafei, *Mater. Chem. Phys.* 105 (2007) 105.
23. H. Lgaz, A. Chaouiki, M.R. Albayati, R. Salghi, Y. El Aoufir, I.H. Ali, M.I. Khan, S.K. Mohamed, I.-M. Chung, *Res. Chem. Intermed.* 45 (2019) 2269.
24. E.-S.M. Sherif, A.H. Ahmed, *Synth. React. Inorg. Met.-Org. Nano-Met. Chem.* 40 (2010) 365.
25. H. Lgaz, I.-M. Chung, M.R. Albayati, A. Chaouiki, R. Salghi, S.K. Mohamed, *Arab. J. Chem.* In press (2018). doi:10.1016/j.arabjc.2018.08.004.
26. H. Lgaz, I.-M. Chung, R. Salghi, I.H. Ali, A. Chaouiki, Y. El Aoufir, M.I. Khan, *Appl. Surf. Sci.* 463 (2019) 647.
27. J. Scully, R. Baboian, *ASTM Phila. PA.* (1995) 110.
28. ASTM Committee G-1 on Corrosion of Metals, Standard practice for preparing, cleaning, and evaluating corrosion test specimens, *ASTM International*, 2011.
29. Z. Salarvand, M. Amirnasr, M. Talebian, K. Raeissi, S. Meghdadi, *Corros. Sci.* 114 (2017) 133.
30. M. Yadav, R.R. Sinha, T.K. Sarkar, N. Tiwari, *J. Adhes. Sci. Technol.* 29 (2015) 1690.
31. J. Tkacz, J. Minda, S. Fintová, J. Wasserbauer, *Materials*, 9 (2016) 925.
32. C. Verma, M.A. Quraishi, A. Singh, *J. Mol. Liq.* 212 (2015) 804.
33. M. Hegazy, A. Badawi, S.A. El Rehim, W. Kamel, *Corros. Sci.* 69 (2013) 110.
34. F. Bentiss, M. Lebrini, H. Vezin, M. Lagrenée, *Mater. Chem. Phys.* 87 (2004) 18.
35. M. Parveen, M. Mobin, S. Zehra, *RSC Adv.* 6 (2016) 61235.
36. H. Lgaz, R. Salghi, S. Jodeh, B. Hammouti, *J. Mol. Liq.* 225 (2017) 271.
37. Y. Sasikumar, A.S. Adekunle, L.O. Olasunkanmi, I. Bahadur, R. Baskar, M.M. Kabanda, I.B. Obot, E.E. Ebenso, *J. Mol. Liq.* 211 (2015) 105.
38. K. Krishnaveni, J. Ravichandran, *J. Electroanal. Chem.* 735 (2014) 24.
39. M. El Azhar, B. Mernari, M. Traisnel, F. Bentiss, M. Lagrenee, *Corros. Sci.* 43 (2001) 2229.
40. A. Yurt, A. Balaban, S.U. Kandemir, G. Bereket, B. Erk, *Mater. Chem. Phys.* 85 (2004) 420.
41. K. Azzaoui, E. Mejdoubi, S. Jodeh, A. Lamhamdi, E. Rodriguez-Castellón, M. Algarra, A. Zarrouk, A. Errich, R. Salghi, H. Lgaz, *Corros. Sci.* 129 (2017) 70.
42. L.O. Olasunkanmi, I.B. Obot, E.E. Ebenso, *RSC Adv.* 6 (2016) 86782.
43. M. Gholami, I. Danaee, M.H. Maddahy, M. RashvandAvei, *Ind. Eng. Chem. Res.* 52 (2013) 14875.
44. Z. Salarvand, M. Amirnasr, M. Talebian, K. Raeissi, S. Meghdadi, *Corros. Sci.* 114 (2017) 133.
45. M. Lebrini, F. Bentiss, H. Vezin, M. Lagrenee, *Corros. Sci.* 48 (2006) 1279.
46. S. Pareek, D. Jain, S. Hussain, A. Biswas, R. Shrivastava, S.K. Parida, H.K. Kisan, H. Lgaz, I.-M. Chung, D. Behera, *Chem. Eng. J.* 358 (2019) 725.
47. A. Singh, K.R. Ansari, M.A. Quraishi, H. Lgaz, Y. Lin, *J. Alloys Compd.* 762 (2018) 347.

48. A. Singh, K.R. Ansari, J. Haque, P. Dohare, H. Lgaz, R. Salghi, M.A. Quraishi, *J. Taiwan Inst. Chem. Eng.* 82 (2018) 233.
49. N. Saini, R. Kumar, H. Lgaz, R. Salghi, I.-M. Chung, S. Kumar, S. Lata, *J. Mol. Liq.* 269 (2018) 371.
50. D.I. Njoku, Y. Li, H. Lgaz, E.E. Oguzie, *J. Mol. Liq.* 249 (2018) 371.
51. D.S. Chauhan, K.R. Ansari, A.A. Sorour, M.A. Quraishi, H. Lgaz, R. Salghi, *Int. J. Biol. Macromol.* 107 (2018) 1747.
52. S. Dubey, S. Banerjee, S.N. Upadhyay, Y.C. Sharma, *J. Mol. Liq.* 240 (2017) 656.
53. A.K. Singh, S. Thakur, B. Pani, B. Chugh, H. Lgaz, I.-M. Chung, P. Chaubey, A.K. Pandey, J. Singh, *J. Mol. Liq.* 283 (2019) 788.
54. N. Chafai, S. Chafaa, K. Benbouguerra, A. Hellal, M. Mehri, *J. Mol. Struct.* 1181 (2019) 83.
55. B. Liu, H. Xi, Z. Li, Q. Xia, *Appl. Surf. Sci.* 258 (2012) 6679.
56. M. Abdallah, A. s. Fouda, S. a. EL-Sayyad, *Anti-Corros. Methods Mater.* 58 (2011) 63.
57. A.S. Fouda, G.E. Badr, M.N. El-Haddad, *J. Korean Chem. Soc.* 52 (2008) 124.
58. A.M.A. Alaghaz, R.A.A. Ammar, *Phosphorus Sulfur Silicon Relat. Elem.* 183 (2008) 2827.
59. N. Chafai, S. Chafaa, K. Benbouguerra, A. Hellal, M. Mehri, *J. Mol. Struct.* 1181 (2019) 83.
60. D.K. Singh, E.E. Ebenso, M.K. Singh, D. Behera, G. Udayabhanu, R.P. John, *J. Mol. Liq.* 250 (2018) 88.